Inorg. Chem. **2006**, *45*, 3275–3280

Hybrid Organic–Inorganic Conductor with a Magnetic Chain Anion: κ-BETS$_2$[Fe^{III}(C$_2$O$_4$)Cl$_2$] [BETS = Bis(ethylenedithio)tetraselenafulvalene]

Bin Zhang,*,† Zheming Wang,‡ Yan Zhang,§ Kazuyuki Takahashi,¶ Yoshinori Okano,¶ Hengbo Cui,¶ Hayao Kobayashi,*,¶ Katsuya Inoue,# Mohamedally Kurmoo,|| Francis L. Pratt,⊥ and Daoben Zhu*,†

Organic Solid Laboratory, CMS, Institute of Chemistry, The Chinese Academy of Sciences, Beijing 100080, People's Republic of China, The College of Chemistry and Molecular Engineering, Peking University, Beijing 100871, People's Republic of China, The College of Physics, Peking University, Beijing 100871, People's Republic of China, Institute for Molecular Science and CREST, JST, Okazaki 444-8585, Japan, Department of Chemistry, Faculty of Science, Hiroshima University, Kagamiyama, Higashi Hiroshima 739-8526, Japan, Laboratoire de Chimie de Coordination Organique, CNRS-UMR7140, Université Louis Pasteur, 4 rue Blaise Pascal, 67000 Strasbourg Cedex1, France, and Rutherford Appleton Laboratory, Chilton, Didcot OX11 0QX, U.K.

Received October 27, 2005

The synthesis, crystal structure, and electrical, optical, and magnetic properties of κ-BETS$_2$[Fe^{III}(C$_2$O$_4$)Cl$_2$], where BETS is bis(ethylenedithio)tetraselenafulvalene, are reported. The black plate crystals consist of parallel donor layers, two per unit cell, displaying a κ-type packing of BETS$^{0.5+}$ within the *bc* plane and anionic magnetic chains, [Fe(C$_2$O$_4$)Cl$_2^-$]$_n$, running along the *c* axis. It displays metallic behavior down to 4.2 K, and analysis of the optical reflectivity data gives unscreened plasma energies of 0.69 eV ($E \parallel c$) and 0.40 eV ($E \perp c$). The optical anisotropy is larger than that seen for other κ phases and is described well by transfer integrals obtained from extended Hückel calculations. However, the transfer integrals need to be scaled down uniformly by a factor of 1.21 to reproduce the absolute experimental plasma frequencies. The band structure consists of a one-dimensional (1D) band and a hole pocket, characteristics of κ phases. The magnetic properties were modeled by the sum of a 1D antiferromagnetic chain contribution from the d spins of Fe^{3+}, a temperature-independent paramagnetic contribution, and a Curie impurity term. At 4.5 K, there is a signature of long-range magnetic ordering to a canted-antiferromagnetic state in the zero-field-cooled–field-cooled magnetizations, and at 2 K, a small hysteresis loop is observed.

Introduction

Conducting and magnetic molecular materials are of current interest in the field of functional materials. This interest is due to the cooperative phenomena involving the conducting building blocks (π electron) and the magnetic molecular building blocks (d electron). Consequently, this has driven the development of various organic and inorganic molecular building blocks, whereby their assemblage in the solid-state forms has produced exotic physics.[1] Over the past 15 years, several groups have been interested in combining organic donors and paramagnetic anions in the formation of organic−inorganic hybrids, especially in the search for combined electrical, magnetic, and optical properties, as multifunctional materials potentially used for molecular electronic devices. Organic moieties such as tetrathiafulvalene (TTF) and its derivatives with their π electrons delocalized over the molecule interact through strong orbital overlap between neighboring molecules to form electronic bands, which are responsible for electrical conductivity and Pauli paramagnetism. For semiconducting compounds, the magnetic properties take the form of long-range antiferromagnetism, canted antiferromagnetism, or ferromagnetism.

* To whom correspondence should be addressed. E-mail: zhangbin@iccas.ac.cn (B.Z.), hayao@ims.ac.jp (H.K.), zhudb@iccas.ac.cn (D.Z.). Phone: 8610-62558982 (B.Z. and D.Z.), 81-564-54-2254 (H.K.). Fax: 8610-62559373 (B.Z. and D.Z.), 81-564-54-2254 (H.K.).

† The Chinese Academy of Sciences.

‡ The College of Chemistry and Molecular Engineering, Peking University.

§ The College of Physics, Peking University.

¶ Institute for Molecular Science and CREST, JST.

Hiroshima University.

|| Université Louis Pasteur.

⊥ Rutherford Appleton Laboratory.

(1) For example, see: *Chem. Rev.* **2004**, 104.

10.1021/ic051870q CCC: $33.50 © 2006 American Chemical Society
Published on Web 03/17/2006

For conducting salts, canted antiferromagnetism, long-range antiferromagnetism, metamagnetism, and ferromagnetism have been observed so far.[2] Introduction of inorganic coordination complexes carrying magnetic moments into these salts results in the possible magnetic exchange through π and d spins.[3] The chemistry of hybrids with coordination complexes has so far focused on anions having simple tetrahedral, octahedral, linear, and planar geometries as well as the clusters of Keggin and Dawson,[4] extended polymeric anions such as mercury halides and copper dicyanamide halides, and later the introduction of infinite metal−oxalate layers and extended oxalate anions.[2,5] Early this year, we reported the first compound of TTF with an oxalate-bridged iron chloride linear chain, TTF[$Fe(C_2O_4)Cl_2$],[6] where the polymeric $[Fe(C_2O_4)Cl_2^-]_n$ is an intermediate between a discrete tetrahedral $FeCl_4^-$ anion and two-dimensional (2D) oxalate anions: $[AFe(C_2O_4)_3^{2-}]_n$ (A = K^+, NH_4^+, and H_3O^+) and $[M^{II}M^{III}(C_2O_4)^-]_n$.[2,5] It exhibits intrachain antiferromagnetic $Fe^{3+}\cdots Fe^{3+}$ interactions and π−d interactions through the short contacts between π-donor molecules and the Fe chain. It was found to display long-range antiferromagnetic ordering at an unexpectedly high temperature of 19.8 K. However, this compound is an insulator. Here, we report the first conducting organic−inorganic hybrid system containing this one-dimensional (1D) polymeric anion $[Fe(C_2O_4)Cl_2^-]_n$ and the organic donor bis(ethylenedithio)tetraselenafulvalene (BETS), where π-electron conduction and 1D antiferromagnetism coexist.

Experimental Section

Synthesis. The crystals of **1** were synthesized by the electrocrystallization method as follows. A total of 38 mg of $(Me_4N)_3[Fe(C_2O_4)_3]$ was dissolved in a mixture of 20 mL of C_6H_5Cl and 5 mL of C_2H_5OH and placed in an H cell. A total of 5.2 mg of BETS was placed in the cathodic compartment.[7] The solution in an H cell was subjected to a constant voltage of 3.0 V for 3 weeks at room temperature. Shiny black thin-plate crystals of **1** were obtained on the cathode, together with some κ-$BETS_2FeCl_4$ crystals as a byproduct. The elemental analyses performed by an electron probe microanalyzer gave a composition with a ratio S:Se:Fe:O:Cl of 8:8:1:4:2 as found by X-ray analysis of **1**. Similar analyses on the κ-$BETS_2FeCl_4$ crystals are as follows: S:Se:Fe:Cl of 8:8:1:4.

Table 1. Crystallographic Data of **1**

	1
empirical formula	$C_{22}H_{16}Cl_2FeO_4S_8Se_8$
fw	1359.26
T (K)	293
wavelength (Å)	0.710 73
cryst syst	monoclinic
space group	$C2/c$
a (Å)	37.884(5)
b (Å)	11.258(2)
c (Å)	8.469(1)
β (deg)	90.573(2)
V (Å^3)	3611.8(10)
Z	4
D_c (g cm^{-3})	2.500
μ(Mo Kα) (mm^{-1})	9.123
no. of reflns	18 827 (measd), 4128 (unique), 2864 [$I \geq 2\sigma(I)$]
no. of param	204
R_{int}	0.0578
wR2	0.1090
R1	0.0393
GOF	0.984
residual (e A^{-3}) (min, max)	−0.871, +1.011

A single crystal of dimensions 0.15 × 0.09 × 0.01 mm^3 was mounted for data collection at room temperature on a Rigaku AFC8 mercury CCD diffractometer equipped with a confocal mirror. Monochromated Mo Kα (λ = 0.710 73 Å) radiation was used. The data were corrected for Lorentz and polarization and finally for absorption using an empirical method.[8] The structure was solved by direct methods, and all of the non-H atoms were refined anisotropically by the full-matrix method.[9] The crystallographic data are listed in Table 1. Data have been deposited at the Cambridge Data Center (CCDC 280931).

Specular reflectance spectra were recorded in the range 6500−700 cm^{-1} using a Bio-rad FTS6000 spectrometer equipped with a UMA500 microscope and a Au wire grid on KRS-5 as a polarizer. A Au mirror was used as the reference.

The measurement of the resistance as a function of the temperature from 4.2 to 300 K was carried out on a single crystal by a four-probe method with 15-μm Au wires attached by Au paste. The resistance was that of the most conducting direction of the *bc* plane.

Magnetization measurements were performed on a MPMS SQUID in various applied fields (up to ±70 kOe) and temperatures (1.9−300 K). The sample, consisting of 0.47 mg of individually selected crystals, was placed in aluminum foil. The as-measured data were finally corrected for the contributions from the signal of aluminum and for the diamagnetism of the elements using Pascal's constants.[10]

For the resistance and magnetization measurements, each crystal used was selected on criteria based on its optical reflectivity. We

(2) (a) Akutsu, H.; Arai, E.; Kobayashi, H.; Tanaka, H.; Kobayashi, A.; Cassoux, P. *J. Am. Chem. Soc.* **1997**, *119*, 12681. (b) Ojima, E.; Fujiwara, H.; Kato, K.; Kobayashi, H.; Tanaka, H.; Kobayashi, A.; Tokumoto, M.; Cassoux, P. *J. Am. Chem. Soc.* **1999**, *121*, 5581. (c) Coronado, E.; Galan-Mascaros, J. R.; Gomez-Garcia, C. J.; Laukhin, N. V. *Nature* **2000**, *408*, 447. (d) Uji, S.; Shinagawa, H.; Herashima, T.; Yakabe, T.; Terai, Y.; Tokumoto, M.; Kobayashi, A.; Kobayashi, H. *Nature* **2001**, *410*, 908. (e) Fujiwara, H.; Fujiwara, E.; Nakazawa, Y.; Narymbetov, B. Zh.; Kato, K.; Kobayashi, H.; Kobayashi, A.; Tokumoto, M.; Cassoux, P. *J. Am. Chem. Soc.* **2001**, *123*, 306. (f) Zhang, B.; Tanaka, H.; Fujiwara, H.; Kobayashi, H.; Fujiwara, E.; Kobayashi, A. *J. Am. Chem. Soc.* **2002**, *124*, 9982. (g) Alberola, A.; Coronado, E.; Galan-Mascaros, J. R.; Gimenez-Saiz, C.; Gomez-Garcia, C. J. *J. Am. Chem. Soc.* **2003**, *125*, 10774. (h) Fujiwara, H.; Wada, K.; Hiraoka, T.; Hayashi, T.; Sugimoto, T.; Nakazumi, H.; Yokogawa, K.; Teramura, M.; Yasuzuka, S.; Murata, K.; Mori, T. *J. Am. Chem. Soc.* **2005**, *127*, 14166.

(3) (a) Kagawa, F.; Itou, T.; Miyagawa, K.; Kanoda, K. *Phys. Rev. Lett.* **2000**, *93*, 127001. (b) Kagawa, F.; Miyagawa, K.; Kanoda, K. *Nature* **2005**, *436*, 534.

(4) (a) Coronado, E.; Galan-Mascaros, J. R.; Gimenez-Saiz, C.; Gomez-Garcia, C. J.; Laukhim, V. N. *Adv. Mater.* **1996**, *8*, 801. (b) Coronado, E.; Galan-Mascaros, J. R.; Gimenez-Saiz, C.; Gomez-Garcia, C. J.; Martinez-Ferrero, E.; Almeida, M.; Lopes, E. B. *Adv. Mater.* **2004**, *16*, 324.

(5) Kurmoo, M.; Graham, A. W.; Day, P.; Coles, S. J.; Hursthouse, M. B.; Caulfield, J. L.; Singleton, J.; Pratt, F. L.; Hayes, W.; Ducasse, L.; Guionneau, P. *J. Am. Chem. Soc.* **1995**, *117*, 11209.

(6) Zhang, B.; Wang, Z. M.; Fujiwara, H.; Kobayashi, H.; Kurmoo, M.; Inoue, K.; Mori, T.; Gao, S.; Zhang, Y.; Zhu, D. B. *Adv. Mater.* **2005**, *17*, 1988.

(7) Courcet, T.; Malfant, I.; Pokhodnia, K.; Cassoux, P. *New J. Chem.* **1998**, 585.

(8) Higashi, T. *Absor—Empirical absorption Correction based on Fourier Series Approximation*; Rigaku Corp.: Tokyo, Japan, 1995.

(9) Sheldrick, G. M. *SHELXL-97*; University of Göttingen: Göttingen, Germany, 1997.

(10) Kahn, O. *Molecular Magnetism*; Wiley-VCH: Weinheim, Germany, 1993; p 104.

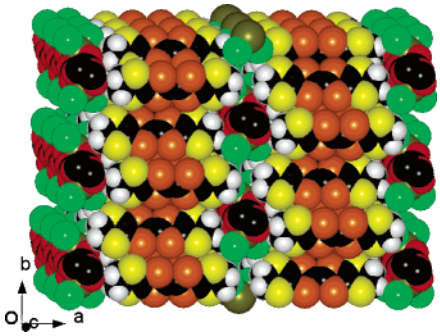

Figure 1. Structure of κ-$BETS_2[Fe(C_2O_4)Cl_2]$: a space-filling view of the packing of BETS layers and $[Fe(C_2O_4)Cl_2^-]_n$ chains in the crystal, viewed along the *c* axis. Color scheme: C, black; H, white; O, red; S, yellow; Cl, green; Fe, brown-green; Se, orange.

selected only crystals showing the presence of oxalate vibrational bands and having a high reflectance. By doing so, we ensured that no κ-$BETS_2FeCl_4$ crystals were present in our samples.

Results and Discussion

Synthesis. The crystals were reproducibly obtained by the above method, though the yield of the two phases varies. Both phases have anion compositions that do not correspond to that of the starting electrolyte, $(Me_4N)_3[Fe(C_2O_4)_3]$. It appears that Cl^- in the anion has its source from the solvent, C_6H_5Cl. Such an observation was first made in the identification of the chloride salt of bis(ethylenedithio)tetrathiafulvalene (BEDT TTF), $(BEDT\ TTF)_3Cl_2(H_2O)_2$.[11] We are presently unable to optimize the conditions to favor either of the phases. It should be pointed out that the ligand field strength is much larger for oxalate compared to chloride. Under the conditions of the present electrocrystallization, it appears that chloride is unexpectedly favored over oxalate. The results indicate that the stability of the crystals with $[Fe(C_2O_4)Cl_2]^-$ or $[FeCl_4]^-$ as counterions is more favorable compared to that with $[Fe(C_2O_4)_3]^{3-}$.

Crystal Structures. The crystal belongs to a monoclinic system (Table 1). The bond lengths and angles are given in Table S1 of the Supporting Information. There is one BETS molecule and half of one $[Fe(C_2O_4)Cl_2^-]$ per asymmetric unit. The structure consists of two parallel BETS layers arranged in the *ab* plane within one unit cell, separated by chains of $[Fe(C_2O_4)Cl_2^-]_n$ running along the *c* axis, as shown in Figure 1. The arrangement of the donors within one layer (Figure 2a) is closely related to that of κ-$BETS_2FeCl_4$ with nearly orthogonal dimers but with slight variations between the dimers and also has the long axis of the molecules in adjacent layers nearly parallel to the *a* axis.[12] Except for the two peripheral ethylene groups, all of the atoms in a donor molecule are coplanar, with a maximum deviation of 0.119 Å from the mean plane. There are Se···Se contacts within the dimer and Se···S contacts between dimers. The dihedral angle between donors of nearest-neighboring pairs is 76.36(2)°. The bond lengths (Table 2) of the TSeF core are in the range found for κ-$BETS_2FeCl_4$ and λ-$BETS_2FeCl_4$,[12] so we can

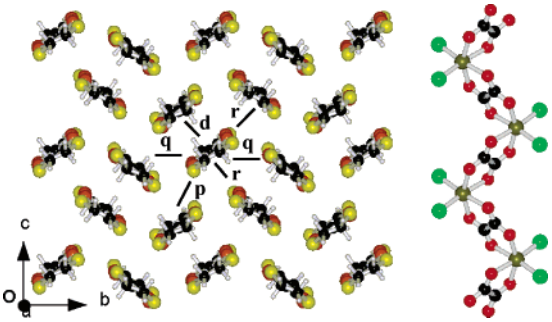

Figure 2. (a) BETS layer showing the κ-type packing of the donors with the definition of the overlap integrals. (b) $[Fe(C_2O_4)Cl_2^-]_n$ chain, viewed along the *a* axis.

assume the formal charge of BETS to be +0.5 and the anion unit $[Fe(C_2O_4)Cl_2^-]_n$ for Fe^{3+}.

The inorganic anion (Figure 2b) is a 1D polymer consisting of Fe^{III} bridged by oxalate dianions in cis positions and two terminal Cl atoms per Fe, as found in $TTF[Fe(C_2O_4)Cl_2]$.[6] Fe−O and Fe−Cl bond lengths are similar to those reported in the literature for oxalate-bridged Fe^{III} complexes and tetrahedral and octahedral coordination anions containing the Fe^{III}−Cl unit.[2,5,6,12,13] The dihedral angle of adjacent oxalate groups of 98.7(2)°, the intrachain Fe···Fe distance of 5.447 Å, and the intrachain Fe···Fe···Fe angle of 102.0° (Figure 2b) are significantly different from those values, 89.8°, 5.494 Å, and 108.0°, in $TTF[Fe^{III}(C_2O_4)Cl_2]$, demonstrating the flexibility in the geometry of the $[Fe(C_2O_4)Cl_2^-]_n$ chain in order to match cations of different sizes and arrangements.

There are several nonbonded interactions, S···Cl, C−H···Cl, and C−H···O, between the donor and anion such as S···Cl: 3.659(3) and 3.561(2) Å. These may induce the π−d interaction between the donor and anion, as found for κ-$BETS_2FeBr_4$ and κ-$BETS_2FeCl_4$.[2,12]

Band Structure. The band structure was calculated using a tight-binding approach from transfer integrals obtained by the extended Hückel method.[14] The definitions of the overlap integrals between highest occupied molecular orbitals (HOMOs) on adjacent molecules and their values are given in Figure 2 and Table 3, respectively. The overlap integrals were calculated for only one BETS layer, given that the two layers within the unit cell are equivalent by symmetry. The inorganic anions were not considered. The overlap integrals are found to have a wide range of values from negative to positive, including some of nearly zero, depending on the orientations and dispositions of both the S and Se π orbitals of adjacent molecules. A simple extended Hückel approximation, $t = -E_IS$, was adopted, where *t* is the transfer integral, *S* is the intermolecular overlap integral of HOMOs, and E_I is the constant, usually taken to be about 10 eV. The dispersions of the four bands are shown in Figure 3a. The overall band structure is similar to that of other κ phases of both BEDT-TTF and BETS. The average charge of $^1/_2e^+$ per BETS results in a $^3/_4$ filling of the bands and a Fermi surface consisting of a 1D section running along the c^* axis

(11) Rosseinsky, M. J.; Kurmoo, M.; Talham, D. R.; Day, P.; Chasseau, D.; Watkin, D. *J. Chem. Soc., Chem. Commun.* **1988**, 88.
(12) Kobayashi, H.; Tomita, H.; Naito, T.; Kobayashi, A.; Sakai, F.; Watanabe, T.; Cassoux, P. *J. Am. Chem. Soc.* **1996**, *118*, 368.
(13) Armemtano, D.; Munno, G. D.; Mastropirtro, T. F.; Julve, M.; Lloret, F. *J. Am. Chem. Soc*. **2005**, *127*, 10778.
(14) Mori, T.; Kobayashi, A.; Sasaki, Y.; Kobayashi, H.; Saito, G.; Inokuchi, H. *Bull. Chem. Soc. Jpn.* **1988**, *57*, 627.

Table 2. Comparison of the Bond Lengths of the TSeF Core in the Complexes of BETS

a, b, c, d were defined as follows

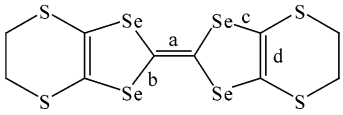

compound	a	d	b	c
λ-$BETS_2GaCl_4$	1.34(1)	1.33(2)	1.878(9), 1.896(9)	1.918(9), 1.905(9)
	1.35(1)	1.33(1)	1.898(10), 1.87(1)	1.892(8), 1.892(8)
		1.33(1)	1.896(10), 1.898(10)	1.891(9), 1.880(8)
		1.32(2)	1.869(9), 1.878(9)	1.910(8), 1.905(8)
λ-$BETS_2FeCl_4$	1.360(7)	1.364(7)	1.897(5), 1.891(5)	1.898(5), 1.888(5)
	1.370(7)	1.361(7)	1.878(5), 1.876(5)	1.896(5), 1.898(5)
		1.358(7)	1.871(5), 1.872(5)	1.894(4), 1.892(5)
		1.343(7)	1.890(4), 1.889(4)	1.892(5), 1.905(5)
κ-$BETS_2GaCl_4$	1.44(3)	1.35(3), 1.31(3)	1.85(2), 1.88(2)	1.89(3), 1.87(2)
			1.85(2), 1.87(2)	1.89(2), 1.91(2)
κ-$BETS_2FeCl_4$	1.358(5)	1.342(5)	1.890(3), 1.884(4)	1.905(4), 1.893(4)
		1.340(5)	1.891(3), 1.887(3)	1.909(3), 1.876(4)
κ-$BETS_2[Fe(C_2O_4)Cl_2]$	1.369(6)	1.352(7)	1.876(4), 1.877(4)	1.901(4), 1.886(5)
		1.337(6)	1.882(4), 1.886(4)	1.898(4), 1.889(5)

Table 3. Overlap Integrals Multiplied by 1000 for **1**, along with Those of κ-$BETS_2FeCl_4$ for Comparison

	d	p	q	r
κ-$BETS_2Fe(C_2O_4)Cl_2$	37.75	17.73	−9.64	0.27
κ-$BETS_2FeCl_4$	32.79	25.05	−9.24	7.92

and a 2D pocket, as shown in Figure 3b. For this Fermi surface, one expects a metallic behavior. Compared with κ-$BETS_2FeCl_4$, the main difference is the very small value for *r* (Table 3), which reduces the dispersion in the *b* direction and makes the band structure more anisotropic. As a result, the 2D pocket is predicted to be significantly larger than that in other κ phases, representing 25% of the Brillouin zone area here, compared with 21% in the other κ phases.

Optical Reflectivity. The IR reflectivity (Figure 4) of **1** is characterized by a plasma edge in the region of 4000 cm^{-1} and sharp vibrational bands at 1270 and 1360 cm^{-1}, originating from the central C═C bonds of the BETS, and sharper ones for the oxalate ions at 1600 and 1684 cm^{-1}. The latter bands are characteristic of **1** and help in separating this phase from that of κ-$BETS_2FeCl_4$. There is considerable anisotropy within the *bc* plane. The data were fitted to the standard Drude−Lorentz model[15] including sharp Lorentzian phonon terms and broad Lorentzian interband terms alongside the intraband Drude term to extract the unscreened optical plasma frequencies for each orientation. The plasma frequencies ω_p and intraband damping rates γ are listed in Table 4, alongside those for some other κ-phase salts, and these are compared with the plasma frequencies derived from band-structure calculations.[16,17] It is found that the absolute values of the transfer integrals need to be reduced by about 20% to match the measured plasma frequencies [$E_I \approx 8.3$ eV (see Figure 3)]. Table 5 lists the optical anisotropy, conductivity, and conductivity anisotropy values derived from the fitted optical parameters. The measured optical anisotropy fits very well to that calculated from the band structure and confirms the enhanced anisotropy of **1** compared to other κ phases. A further indication of the strong electronic anisotropy in this system is the anisotropy of the intraband scattering rate γ, which is significantly lower in the *c* direction than in the *b* direction and lower than either direction in the other κ phases. It is likely that π−d interaction makes a significant contribution to this enhanced scattering rate anisotropy. The conductivity in the *bc* plane is predicted to have an anisotropy

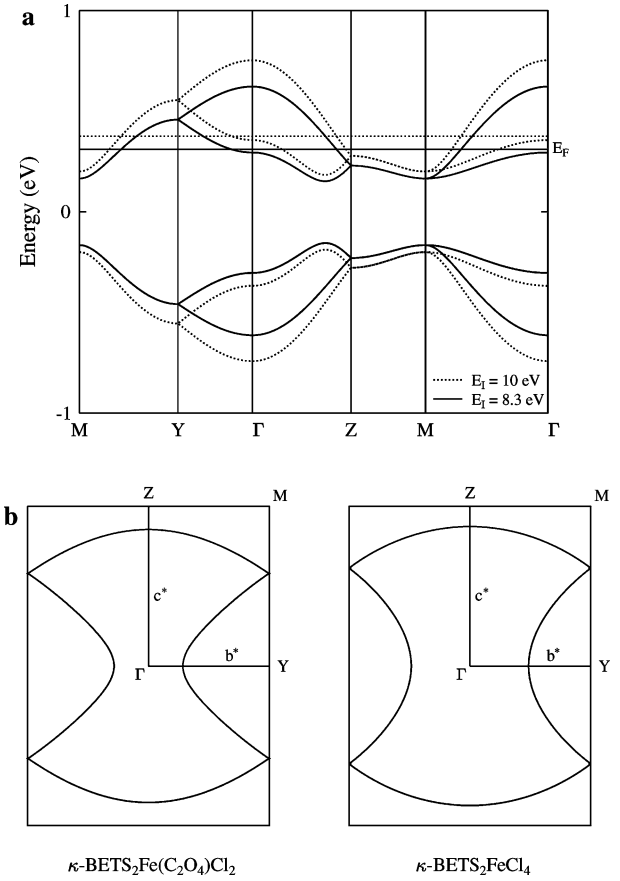

Figure 3. (a) Band structure and (b) Fermi surface for **1** calculated on the basis of the overlap integrals listed in Table 3. In part a, band dispersions are shown for ionization energy values of 10 and 8.3 eV. In part b, the Fermi surface is shown alongside that of κ-$BETS_2FeCl_4$.

(15) Dressel, M.; Drichko, N. *Chem. Rev.* **2004**, *104*, 5689.
(16) Kornelsen, K.; Eldridge, J. E.; Holmes, C. C.; Wang, H. H.; Williams, J. M. *Solid State Commun.* **1989**, *72*, 475.
(17) Oshima, K.; Mori, T.; Inokuchi, H.; Urayama, H.; Yamochi, H.; Saito, G. *Phys. Rev. B* **1988**, *38*, 938.

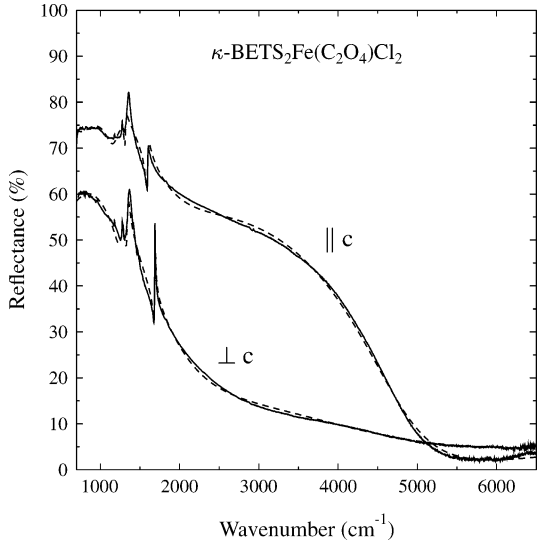

Figure 4. Polarized IR reflectivity measured at room temperature for κ-$BETS_2Fe(C_2O_4)Cl_2$. The dashed lines show Drude−Lorentz fits.

Table 4. Electronic Properties Derived from a Drude−Lorentz Fitting of the IR Reflectivity of **1** and Some Other κ Phases, Compared with the Results of Band-Structure Calculations

		ω_p measd		ω_p calcd, eV	ω_p calcd (scaled), eV	γ, 10^3 cm^{-1}
		10^3 cm^{-1}	eV			
κ-$BETS_2Fe(C_2O_4)Cl_2$	$E \parallel c$	5.55(3)	0.69	0.81	0.67[a]	0.34(2)
	$E \perp c$	3.21(6)	0.40	0.49	0.41[a]	1.11(6)
κ-$BETS_2FeCl_4$	$E \parallel c$	6.56(1)	0.81	0.89	0.79[b]	0.60(1)
	$E \perp c$	4.58(1)	0.57	0.66	0.59[b]	0.96(1)
κ-$ET_2Cu(NCS)_2$	$E \parallel c$	7.88[c]	0.98[c]	0.98[d]		1.97[c]
	$E \perp c$	8.13[c]	1.01[c]	0.85[d]		1.53[c]

[a] ω_p calculated with the original transfer integrals from Table 3 scaled down by a factor of 1.21 (E_I = 8.3 eV). [b] ω_p calculated with the original transfer integrals from Table 3 scaled down by a factor of 1.27 (E_I = 7.9 eV). [c] IR data from Kornelsen et al.[16] [d] Calculated from transfer integrals of Oshima et al.[17]

Table 5. Optical Anisotropy, Conductivity, and Conductivity Anisotropy Derived from the IR Fitting and Band-Structure Calculations

		optical anisotropy $[(\omega_{p\parallel}/\omega_{p\perp})$ $(d_\perp/d_\parallel)]$ measd	calcd	conductivity $[\sigma_0 = \epsilon_0\omega_p^2/\gamma$, 10^3 S cm$^{-1}]$, calcd	conductivity anisotropy $(\sigma_{0\parallel}/\sigma_{0\perp})$, calcd
κ-$BETS_2Fe(C_2O_4)Cl_2$	$E \parallel c$	2.3	2.2	1.5	10
	$E \perp c$			0.15	
κ-$BETS_2FeCl_4$	$E \parallel c$	2.0	1.9	1.2	3.3
	$E \perp c$			0.36	
κ-$ET_2Cu(NCS)_2$	$E \parallel c$	1.5	1.8	0.53	0.74
	$E \perp c$			0.72	

of 10 here, compared to that of the nearly isotropic κ-$ET_2Cu(NCS)_2$ case (Table 5).

Conductivity. As expected from the optical data and the band structure, the crystal displays metallic behavior from room temperature down to 4.2 K (Figure 5). The conductivity measured in the *bc* plane of a crystal at 300 K is 85 S cm^{-1}, which is somewhat lower than that predicted from the optical measurements. Upon cooling, the resistance gradually decreases from 300 to 50 K, followed by a steeper decrease from 50 to 15 K, and then the resistance reaches a plateau, with $R_{300\,K}/R_{4.2\,K} = 16$. This behavior has been observed for

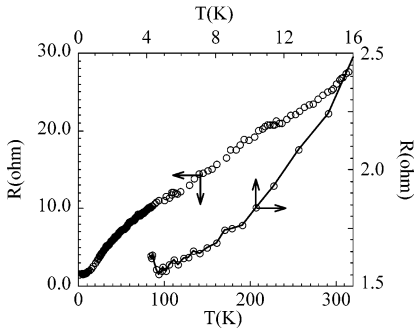

Figure 5. Temperature dependence of the resistance in the *bc* plane.

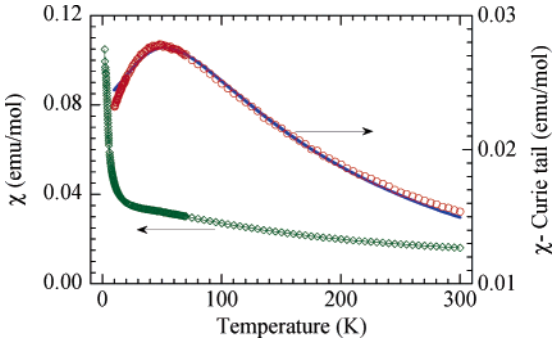

Figure 6. Experimentally observed susceptibility (green diamonds), after correction for the Curie impurity contribution (red circles) and the expected susceptibility for a 1D Heisenberg $S = {}^5/_2$ antiferromagnet (blue line).

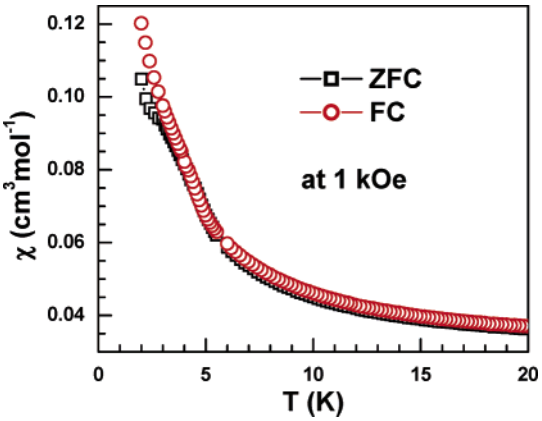

Figure 7. Zero-field-cooled (ZFC) and field-cooled (FC) magnetizations in an applied field of 1 kOe.

many κ-type conductors. This metallic behavior is also expected in view of the calculated band structure and Fermi surface that are characteristic of the κ phase.[12] Below 5 K, there is a slight upturn of 5%. However, further experiments will be needed to confirm this anomaly and whether it is associated with a magnetic long-range ordering.

Magnetic Properties. The magnetization was measured in applied fields of 10^2, 10^3, and 10^4 Oe (1 Oe = $10^3/4\pi$ A m^{-1}) from 2 to 300 K, and data for 10^3 Oe are shown in Figure 6. Upon cooling of the sample, the susceptibility increases to a plateau at around 50 K, followed by an increase below 20 K. Above 100 K, the compound behaves as a Curie−Weiss paramagnet [C = 4.81(2) emu K mol^{-1} and θ = −107 K]. There should be a contribution to the temperature-independent paramagnetism from π metal electrons, but we could not detect it because of the large paramagnetism of Fe^{3+}.[18] The Curie value is close to 4.375

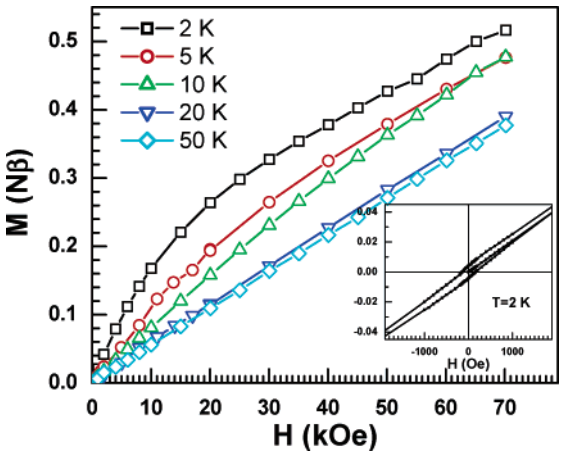

Figure 8. Isothermal magnetization at several temperatures. Inset: small hysteresis loop at 2 K.

emu K mol^{-1} for Fe^{III} ($S = {}^5/_2$). Assuming that the increase below 20 K is due to a Curie impurity, which amounts to a 4% contribution from $S = {}^5/_2$ paramagnetic ions, the susceptibility after correction assumes a broad peak, characteristic of a low-dimensional antiferromagnet. Using the model of Fisher for an antiferromagnetic $S = {}^5/_2$ chain,[19] we simulated the susceptibility for $2J = 25$ K. These values are comparable to those of TTF[Fe(C_2O_4)Cl_2]. At 4.5 K, there is a further magnetic anomaly that may be associated with long-range antiferromagnetic ordering that is seen as a bifurcation in the zero-field-cooled and field-cooled data (Figure 7). To confirm this anomaly, we performed isothermal magnetization measurements at various temperatures. This shows a curvature for low temperatures and has a linear dependence for temperatures above 10 K without any hysteresis or remanant magnetization. At 2 K, a hysteresis loop is observed with a coercive field of $H_c \approx 150$ Oe (Figure 8). The magnetization in 70 kOe is only 10% of that expected if the moments were all aligned parallel. These are characteristic of weak ferromagnetism with a very small canting angle.

Conclusion

κ-BETS$_2$[Fe^{III}(C_2O_4)Cl_2] is an organic−inorganic hybrid that displays the coexistence of 2D π electrons, 1D antiferromagnetism, and possible canted antiferromagnetism involving π and d spins. The metallic nature is predicted by band-structure calculations and confirmed experimentally by resistance and optical measurements. Further exploration of the physical properties of this compound is in progress, in particular fermiology.

Acknowledgment. This research is supported by NSFC Grant Nos. 20473095, 90201014, and CMS-CX200510, in China, the Ministry of Education, in Japan, EPSRC, in the U.K., and the CNRS, in France.

Supporting Information Available: X-ray crystallographic file in CIF format for **1** and a PDF file containing Figures S1−S3. This material is available free of charge via the Internet at http://pubs.acs.org.

IC051870Q

(18) Tanaka, H.; Kobayashi, A.; Sato, A.; Akutsu, H.; Kobayashi, H. *J. Am. Chem. Soc.* **1999**, *121*, 760.
(19) Carlin, R. L. *Magnetochemistry*; Springer-Verlag: Berlin, 1993; p 170.